Fluid Dynamics & Materials Processing FDMP, vol.15, no.5, pp.471-489, 2019

Unsteady MHD Free Convective Flow Past a Vertical Porous Plate with Span-Wise Fluctuating Heat and Mass Transfer Effects

S . Samantha Kumari[1, *] and G. Sankara Sekhar Raju[2]

Abstract: This paper investigates the chemical reaction and thermal radiation effects on unsteady MHD free convective flow past a vertical porous plate in the presence of heat absorption/generation. The novelty of present investigation is that the temperature and concentration of the plate are span wise cosinusoidally unsteady with time. The second order perturbation technique is employed to study the non-linear partial differential equations which govern the fluid flow. The effects of magnetic parameter, radiation, Eckert number, Schmidt number and chemical reaction parameters on velocity, temperature and concentration distributions as well as skin friction coefficients, the rate of heat transfer and the rate of mass transfer are discussed through figures and tables. It is noticed that the Nusselt number declines with rising values of Prandtl and Eckert numbers.

Keywords: MHD, porous medium, thermal radiation, cosinusoidally fluctuating conditions, chemical reaction.

1 Introduction

Simultaneous heat and mass transfer over a vertical plate in the presence of MHD and chemical reaction effects rise in many branches of engineering and industrial applications; resembling the industry, packed bed chemical change reactors, cooling of nuclear reactors, chemical vapor proof on surfaces etc. In view of these industrial applications, Paras Ram et al. [Paras, Hawa, Rakesh et al. (2017)] explored the effects of MHD and radiation on unsteady incompressible fluid past a porous vertical plate in the presence of cosinusoidally heat transfer conditions. Hussain et al. [Hussain, Jain, Seth et al. (2015)] studied the consequences of chemical reaction and Hall currents on an accelerated moving plate in a rotating system. Balla et al. [Balla and Kishan (2015)] studied the influence chemical reaction and viscous dissipation on MHD vertical porous plate with different heat transfer conditions. Das et al. [Das, Guchhait, Jana et al. (2016)] explored the radiative heat transfer and Hall effects on unsteady MHD porous plate. Asma et al. [Asma, Khan and Sharidan (2016)] analyzed the analysis of Ferro-nano particles over a vertical plate with ramped wall temperature. The influence of chemical reaction on MHD

[1] Department of Mathematics, JNTUA, Anantapuramu, India.

[2] Department of Mathematics, JNTUA College of Engineering, Pulivendula, India.

[*] Corresponding Author: S. Samantha Kumari. Email: hkesavulu6@gmail.com.

polar fluid with periodical plate rate was studied by Bakr [Bakr (2011)]. Swathi et al. [Swathi and Iswar (2015)] explored the slip effects over a vertical porous plate in the presence of magnetic field. Venkateswarlu et al. [Venkateshwarlu and Satyanarayana (2015)] studied radiation absorption effects past a vertical plate in a rotating system with chemical reaction.

The study of fluid flows through porous medium with different boundary conditions has attracted many recent researchers because of their applications in chemical industries, spring water pollution, filtration and transpiration cooling, etc. Ahmed et al. [Ahmed and Talukdar (2011)] investigated influence of MHD and periodic suction past a porous plate in the presence of a rotating system. Ravi Kumar et al. [Ravi Kumar, Rajua and Raju (2018)] analyzed the Rivlin-Ericksen flow past a semi-infinite vertical porous plate with variable temperature and suction. Arifuzzaman et al. [Arifuzzaman, Khan, Mehedi et al. (2018)] examined the radiation absorption effects on MHD fluid flow past a vertical porous plate. Mondal et al. [Mondal, Dulal, Sewli et al. (2017)] analyses the thermophoresis and non-uniform heat source/sink effects on MHD inclined plate. The influence of assorted heat and mass transfer effects on different fluid flows in various flow geometries has been studied by Rama et al. [Rama, Krishna Reddyand Raju (2018)], Soid et al. [Soid, Ishak and Pop (2017)], Nayak et al. [Nayak, Dash and Singh (2016)], Muthuraj et al. [Muthuraj, Nirmala and Srinivas (2016)], Seth et al. [Seth, Sharma and Kumbhakar (2016)].

The role of thermal radiation is very important on many advanced energy transformation systems which are operating at higher temperatures. The effects of thermal radiation on the forced and free convection flows are also important in the context of space technology and processes involving high temperatures. In light-weight of those numerous applications, Singh et al. [Singh, Ram and Kumar (2014)] examined the viscous dissipation and thermal radiation effects on unsteady MHD free convection past vertical plate. Makinde et al. [Makinde, Khan and Khan (2016)] analyzed the MHD and chemical reaction effects over a stretching sheet with convective boundary condition. Satya Narayana et al. [Satya Narayana, Akshit, Ghori et al. (2017)], Satya Narayan et al. [Satya Narayan, Tarakaramu, Makinde et al. (2018)], Sarojamma et al. [Sarojamma, Vijaya Lakshmi, Satya Narayana et al. (2018)] examined the thermal radiation effects on unsteady nanofluid flow caused due to the sheet stretching. In their study the monotonically convergent series solution is attained by utilizing Runge-Kutta-Fehlberg algorithm.

The free-surface profile and the spatial and temporal distribution of velocities in real fields is well accounted for by the inviscid solutions, and viscous damping. The large waves can travel across wide ocean basins without great loss of energy. But the predicted nonzero velocities at the solid bottom boundary under the waves is clearly contrary to fact: just as in unidirectional flows of real fluids, the velocity must go to zero at the bottom boundary. This leads to the concept of the bottom boundary layer in oscillatory flows: this is commonly called the wave boundary layer. In view of these applications, Anuradha [Anuradha (2014)] studied the influence of cosinusoidally unsteady temperature on MHD flow past an infinite vertical porous plate. Nandkeolyar et al. [Nandkeolyar and Das (2013)] mentioned the influence of ramped wall temperature past a flat plate. Seth et al. [Seth, Sarkar and Hussain (2014)] examined the radiation and Hall current effects past a moving vertical plate. The

influence of assorted heat and mass transfer effects on completely different flow geometries with different fluids are studied by Chamkha et al. [Chamkha, Mohamed and Ahmed (2011); Ahmed, Zueco and Lopez-Gonzalez (2017); Seshaiahand and Varma (2016); Rana, Mehmood, Narayana et al. (2016); Harish Babu and Satya Narayana (2016); Satya Narayana and Harish Babu (2013)].

In spite of all the previous studies the attention paid by the researchers towards the influence of variable temperature and concentration on unsteady MHD free convection flow past a vertical plate is scant. Hence, the objective of this work is to analyze the effects of thermal radiation, chemical reaction and heat source past an infinite vertical porous plate. The governing equations are solved by the regular perturbation method. The influence of different flow parameters on the velocity, temperature, concentration, skin-friction, Nusselt number and Sherwood number has been discussed and displayed through graphs and tables.

2 Mathematical formulation

We consider the unsteady incompressible electrically conducting and radiating fluid along porous plate lying vertically on the X^*Z^*plane. The X^*-axis is taken along the direction of buoyancy force and Y^*-axis is normal to the plate as shown in Fig. 1. The cosinusoidel fluctuating temperature and concentration of the plate are assumed to be of the form $T_w^*(z^*,t^*) = T_0^* + \varepsilon(T_0^* - T_\infty^*)\cos(\frac{\pi z^*}{l} - \omega^* t^*)$ and

$$C_w^*(z^*,t^*) = C_0^* + \varepsilon(C_0^* - C_\infty^*)\cos(\frac{\pi z^*}{l} - \omega^* t^*)$$

where T_0^*, T_∞^* *and* T_w^* are the mean, ambient temperature and wall temperature of the plate respectively ω^* is the frequency, t^* is the time, l is the wave length and ε is a small parameter i.e. $\varepsilon \ll 1$. Also, it assumed that the Soret and Dufour effects in the energy equation and the concentrations equation can be ignored, as the level of concentration is usually assembled to be very low in free convections flows.

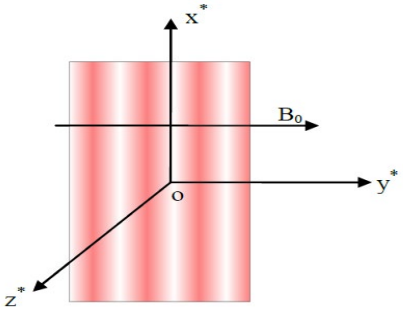

Figure 1: Flow configuration of the problem

The governing equations of momentum, energy and mass including the dissipation function term are given by

$$\frac{\partial v^*}{\partial y^*} = 0 \text{ implies that } \upsilon^* = -V., V > 0 \tag{1}$$

$$\frac{\partial u^*}{\partial t^*} + \upsilon^* \frac{\partial u^*}{\partial y^*} = g\beta\left(T^* - T_\infty\right) + g\beta^*\left(C^* - C_\infty\right) + \upsilon\left[\frac{\partial^2 u^*}{\partial y^{*2}} + \frac{\partial^2 u^*}{\partial z^{*2}}\right] - \alpha\frac{\mu_c^2 H_0^2}{\rho}u^* - \upsilon\frac{u^*}{K^*} \tag{2}$$

$$\rho c_p\left(\frac{\partial T^*}{\partial t^*} + \upsilon^*\frac{\partial T^*}{\partial y^*}\right) = k\left(\frac{\partial^2 T^*}{\partial t^{*2}} + \frac{\partial^2 T^*}{\partial z^{*2}}\right) + \mu\left[\left(\frac{\partial u^*}{\partial y^*}\right)^2 + \left(\frac{\partial u^*}{\partial z^*}\right)^2\right] - \frac{\partial q_r}{\partial y^*} + Q_0\left(T^* - T_\infty\right) \tag{3}$$

$$\frac{\partial C^*}{\partial t^*} + \upsilon^*\frac{\partial C^*}{\partial y^*} = D\left(\frac{\partial^2 C^*}{\partial y^{*2}} + \frac{\partial^2 C^*}{\partial z^{*2}}\right) - K_1\left(C^* - C_\infty\right) \tag{4}$$

The flow is subjected to the boundary conditions:

$$\left.\begin{aligned} &u^* = 0,\ T^* = T_0 + \varepsilon\left(T_0 - T_\infty\right)\cos\left(\frac{\pi z^*}{l} - \omega^* t^*\right),\ C^* = c_0 + \varepsilon(c_0 - c_\infty)\cos(\frac{\pi z^*}{l} - \omega^* t^*) \quad at \quad y^* = 0 \\ &u^* = 0,\ T^* = T_\infty,\ C^* = C_\infty \qquad\qquad as\ y^* \to \infty \end{aligned}\right\} \tag{5}$$

According to Vincenti et al. [Vincenti and Krugger (1965)] the radiative heat flux is defined as:

$$\frac{\partial q_r}{\partial y^*} = 4\sigma_s k_e\left(T*^2 - T_\infty^4\right) \tag{6}$$

Assuming that the differences in temperature within the flow are sufficiently small such that T^4 can be expressed as a linear combination of the temperature about T_∞ as follows:

$$T*^4 \cong 4T_\infty^3 T^* - 3T_\infty^4 \tag{7}$$

In view of Eqs. (6) and (7), Eq. (3) becomes

$$\rho c_p\left(\frac{\partial T^*}{\partial t^*} + \upsilon^*\frac{\partial T^*}{\partial y^*}\right) = k\left(\frac{\partial^2 T^*}{\partial t^{*2}} + \frac{\partial^2 T^*}{\partial z^{*2}}\right) + \mu\left[\left(\frac{\partial u^*}{\partial y^*}\right)^2 + \left(\frac{\partial u^*}{\partial z^*}\right)^2\right]$$
$$-16k_e\sigma_s T_\infty^3\left(T^* - T_\infty\right) + Q_0\left(T^* - T_\infty\right) \tag{8}$$

The non-dimensional parameters are as follows:

$$\left.\begin{aligned} &y=\frac{y^*}{l}, t=\omega^* t^*, u=\frac{u^*}{V}, z=\frac{z^*}{l}, K=\frac{k^*}{l}, \omega=\frac{\omega^* l^2}{\upsilon}, \mathrm{Re}=\frac{vl}{\upsilon}, y=\frac{l^2 k_l}{\upsilon} \\ &Gm=\frac{\upsilon g\,\beta^*\left(C_w-C_\infty\right)}{V^3}, Gr=\frac{\upsilon g\,\beta^*\left(T_0-T_\infty\right)}{V^3}, M^2=\frac{\sigma\mu_e^2 H_0^2 l^2}{\upsilon\rho}, R=\frac{16k_e v^2\sigma_s T_\infty^3}{kV^2} \\ &\mathrm{Pr}=\frac{\mu c_p}{k},\ Sc=\frac{\upsilon}{D},\ Ec=\frac{V^2}{c_p\left(T_0-T_\infty\right)},\ \varphi=\frac{Q_0 l^2}{pc_p\upsilon}, C=\frac{C^*-C_\infty}{C_w-C_\infty}, \theta=\frac{T^*-T_\infty}{T_0-T_\infty} \end{aligned}\right\} \tag{9}$$

In view of Eq. (9) the Eqs. (2), (8) and (4) become:

$$\omega\frac{\partial u}{\partial t}-\mathrm{Re}\frac{\partial u}{\partial y}=\mathrm{Re}^2\left(Gr\theta+GmC\right)+\left(\frac{\partial^2 u}{\partial y^2}+\frac{\partial^2 u}{\partial z^2}\right)-M^2 u-\frac{u}{K} \tag{10}$$

$$\omega\frac{\partial\theta}{\partial t}-\mathrm{Re}\frac{\partial\theta}{\partial y}=\frac{1}{\mathrm{Pr}}\left(\frac{\partial^2\theta}{\partial y^2}+\frac{\partial^2\theta}{\partial z^2}\right)+Ec\left[\left(\frac{\partial u}{\partial y}\right)^2+\left(\frac{\partial u}{\partial z}\right)^2\right]-\frac{\mathrm{Re}^2 R}{\mathrm{Pr}}\theta+\varphi\theta \tag{11}$$

$$\omega\frac{\partial C}{\partial t}-\mathrm{Re}\frac{\partial C}{\partial y}=\frac{1}{Sc}\left(\frac{\partial^2 C}{\partial y^2}+\frac{\partial^2 C}{\partial z^2}\right)-\gamma C \tag{12}$$

The boundary conditions are given by

$$\left.\begin{aligned} &u=0,\theta=1+\varepsilon\cos\left(\pi z-t\right), C=1+\in\cos\left(\pi z-t\right) && at\ y=0; \\ &u=0,\theta=0, C=0 && as\ y\to\infty \end{aligned}\right\} \tag{13}$$

3 Solution of the problem

The solution of partial differential Eqs. (10)-(12) together with the boundary condition Eq. (13) is obtained by using perturbation technique [Chamka (2014)].

We assume,

$$f\left(y,z,t\right)=f_0\left(y\right)+\varepsilon f_1\left(y\right)e^{i(\pi z-t)}+\varepsilon^2 f_2\left(y\right)e^{2i(\pi z-t)} \tag{14}$$

where f stands for u, θ and C.

In view of Eq. (14) the Eqs. (10)-(12) are reduced to (equating the like powers of ε)

Zeroth order equations

$$\frac{d^2 u_0}{dy^2}+\mathrm{Re}\frac{du_0}{dy}-Nu_0=-\mathrm{Re}^2\left(Gr\,\theta_0+Gm\,C_0\right) \tag{15}$$

$$\frac{d^2\theta_0}{dy^2}+\mathrm{Re}\,\mathrm{Pr}\frac{d\theta_0}{dy}-\alpha_2\theta_0+Ec\ \mathrm{Pr}\left(\frac{du_0}{dy}\right)^2=0 \tag{16}$$

$$\frac{d^2C_0}{dy^2} + \mathrm{Re}\,Sc\frac{dC_0}{dy} - \gamma Sc\ C_0 = 0 \tag{17}$$

The corresponding boundary conditions are given by

$$\left.\begin{array}{l} u_0 = 0, \theta_0 = 1, C_0 = 1\ at\ \ y = 0; \\ u_0 = 0, \theta_0 = 0, C_0 = 0\ as\ \ y \to \infty \end{array}\right\} \tag{18}$$

First order equations

$$\frac{d^2u_1}{dy^2} + \mathrm{Re}\frac{du_1}{dy} - \alpha_1 u_1 = -\mathrm{Re}^2\left(Gr\,\theta_1 + Gm\,C_1\right) \tag{19}$$

$$\frac{d^2\theta_1}{dy^2} + \mathrm{Re}\ \mathrm{Pr}\frac{d\theta_1}{dy} - \alpha_3\theta_1 = -2\,\mathrm{Pr}\,Ec\ \frac{du_0}{dy}\ \frac{du_1}{dy} \tag{20}$$

$$\frac{d^2C_1}{dy^2} + \mathrm{Re}\,Sc\frac{dC_1}{dy} - \left(\gamma Sc + \pi^2 - i\omega Sc\right)C_1 = 0 \tag{21}$$

The corresponding boundary conditions reduce to

$$\left.\begin{array}{l} u_1 = 0, \theta_1 = 1, C_1 = 1\ at\ \ y = 0; \\ u_1 = 0, \theta_1 = 0, C_1 = 0\ as\ \ y \to \infty \end{array}\right\} \tag{22}$$

Second order equations

$$\frac{d^2u_2}{dy^2} + \mathrm{Re}\frac{du_2}{dy} - \alpha_4 u_2 = -\mathrm{Re}^2\left(Gr\,\theta_2 + Gm\,C_2\right) \tag{23}$$

$$\frac{d^2\theta_2}{dy^2} + \mathrm{Re}\ \mathrm{Pr}\frac{d\theta_2}{dy} - \alpha_5\theta_2 = -\mathrm{Pr}\,Ec\left[\left(\frac{du_1}{dy}\right)^2 + 2\left(\frac{du_0}{dy}\right)\left(\frac{du_2}{dy}\right)\right] \tag{24}$$

$$\frac{d^2C_2}{dy^2} + \mathrm{Re}\,Sc\frac{dC_2}{dy} - \left(\gamma Sc + 4\pi^2 - 2i\omega Sc\right)C_2 = 0 \tag{25}$$

The corresponding boundary conditions are

$$\left.\begin{array}{l} u_2 = 0, \theta_2 = 0, C_2 = 0\ at\ \ y = 0; \\ u_2 = 0, \theta_2 = 0, C_2 = 0\ as\ \ y \to \infty \end{array}\right\} \tag{26}$$

The expressions for C_0 (y), C_1(y) and C_2(y) are obtained as:

$$C_0(y) = e^{-m1y}, C_1(y) = 0, C_2(y) = 0 \tag{27}$$

Assume that

$$F(y) = F_0(y) + EcF_1(y) + Ec^2\,F_2(y) \tag{28}$$

where F stands for any $u_0, u_1, u_2, \theta_0, \theta_1, \theta_2$.

Substituting Eq. (28) into Eqs. (15), (16), (19), (20) and (23), (24) and equating like powers of Ec, we obtain:

Zeroth order equations

$$u_{00}'' + \mathrm{Re}\, u_{00}' - N u_{00} = -\mathrm{Re}^2 \left(Gr\, \theta_{00} + Gm\, e^{-m1y} \right) \tag{29}$$

$$u_{01}'' + \mathrm{Re}\, u_{01}' - N u_{01} = -\mathrm{Re}^2\ Gr\ \theta_{01} \tag{30}$$

$$u_{02}'' + \mathrm{Re}\, u_{02}' - N u_{02} = -\mathrm{Re}^2\ Gr\ \theta_{02} \tag{31}$$

$$\theta_{00}'' + \mathrm{Re}\ \mathrm{Pr}\, \theta_{00}' - \alpha_2 \theta_{00} = 0 \tag{32}$$

$$\theta_{01}'' + \mathrm{Re}\ \mathrm{Pr}\, \theta_{01}' - \alpha_2 \theta_{01} = -\mathrm{Pr}\, u_{00}'^2 \tag{33}$$

$$\theta_{02}'' + \mathrm{Re}\ \mathrm{Pr}\, \theta_{02}' - \alpha_2 \theta_{02} = -2\,\mathrm{Pr}\, u_{00}' \tag{34}$$

The corresponding boundary conditions are

$$\left.\begin{array}{l} u_{00} = 0,\ \theta_{00} = 1,\ u_{01} = 0,\ \theta_{01} = 0,\ u_{02} = 0, \theta_{02} = 0 \ at\ y = 0; \\ u_{00} = 0,\ \theta_{00} = 0,\ u_{01} = 0,\ \theta_{01} = 0,\ u_{02} = 0, \theta_{02} = 0 \ as\ y \to \infty \end{array}\right\} \tag{35}$$

First order equations are

$$u_{10}'' + \mathrm{Re}\, u_{10}' - \alpha_1 u_{10} = -\mathrm{Re}^2\ Gr\ \theta_{10} \tag{36}$$

$$u_{11}'' + \mathrm{Re}\, u_{11}' - \alpha_1 u_{11} = -\mathrm{Re}^2\ Gr\ \theta_{11} \tag{37}$$

$$u_{12}'' + \mathrm{Re}\, u_{12}' - \alpha_1 u_{12} = -\mathrm{Re}^2\ Gr\ \theta_{12} \tag{38}$$

$$\theta_{10}'' + \mathrm{Re}\,\mathrm{Pr}\, \theta_{10}' - \alpha_3 \theta_{10} = 0 \tag{39}$$

$$\theta_{11}'' + \mathrm{Re}\,\mathrm{Pr}\, \theta_{11}' - \alpha_3 \theta_{11} = -2\,\mathrm{Pr}\, u_{00}' u_{10}' \tag{40}$$

$$\theta_{12}'' + \mathrm{Re}\,\mathrm{Pr}\, \theta_{12}' - \alpha_3 \theta_{12} = -2\,\mathrm{Pr}\left[u_{00}' u_{11}' + u_{01}'\, u_{10}' \right] \tag{41}$$

The corresponding boundary conditions are

$$\left.\begin{array}{l} u_{10} = 0,\ \theta_{10} = 1,\ u_{11} = 0,\ \theta_{11} = 0,\ u_{12} = 0, \theta_{12} = 0 \ at\ y = 0; \\ u_{10} = 0,\ \theta_{10} = 0,\ u_{11} = 0,\ \theta_{11} = 0,\ u_{12} = 0, \theta_{12} = 0 \ as\ y \to \infty \end{array}\right\} \tag{42}$$

Second order equations

$$u_{20}'' + \mathrm{Re}\, u_{20}' - \alpha_4 u_{20} = -\mathrm{Re}^2\ Gr\ \theta_{20} \tag{43}$$

$$u_{21}'' + \mathrm{Re}\, u_{21}' - \alpha_4 u_{21} = -\mathrm{Re}^2\ Gr\ \theta_{21} \tag{44}$$

$$u_{22}'' + \mathrm{Re}\, u_{22}' - \alpha_4 u_{22} = -\mathrm{Re}^2\ Gr\ \theta_{22} \tag{45}$$

$$\theta_{20}'' + \mathrm{Re}\,\mathrm{Pr}\,\theta_{20}' - \alpha_5\theta_{20} = 0 \tag{46}$$

$$\theta_{21}'' + \mathrm{Re}\,\mathrm{Pr}\,\theta_{21}' - \alpha_5\theta_{21} = -\mathrm{Pr}\,2u_{00}'u_{20}' \tag{47}$$

$$\theta_{22}'' + \mathrm{Re}\,\mathrm{Pr}\,\theta_{22}' - \alpha_5\theta_{22} = -\mathrm{Pr}\left[2u_{00}'u_{11}' + 2u_{00}'\,u_{21}' + 2u_{01}'\,u_{20}'\right] \tag{48}$$

The corresponding boundary conditions are

$$\left.\begin{array}{l} u_{20} = 0,\ \theta_{20} = 1,\ u_{21} = 0,\ \theta_{21} = 0,\ u_{22} = 0, \theta_{22} = 0 \ at\ y = 0; \\ u_{20} = 0,\ \theta_{20} = 0,\ u_{21} = 0,\ \theta_{21} = 0,\ u_{22} = 0, \theta_{22} = 0 as\ y \to \infty \end{array}\right\} \tag{49}$$

By solving Eqs. (29)-(34), (36-41) and (43-48) using the boundary conditions (35), (42) and (49) respectively, we get the following set of solutions.

$$u_{00} = B_3e^{-n_{10}y} - B_1e^{-n_8y} - B_2e^{-n_2y}$$

$$\theta_{00} = e^{-n_8y}$$

$$\theta_{01} = B_{16}e^{-n_{12}y} - B_{10}e^{-2n_{10}y} - B_{11}e^{-2n_8y} - B_{12}e^{-2n_2y} + B_{13}e^{-(n_8+n_{10})y} - B_{14}e^{-(n_2+n_8)y} + B_{15}e^{-(n_2+n_{10})y}.$$

$$u_{01} = B_{24}e^{-n_{14}y} - B_{17}e^{-n_{12}y} + B_{18}e^{-2n_{10}y} + B_{19}e^{-2n_8y} + B_{20}e^{-2n_2y} - B_{21}e^{-(n_8+n_{10})y} + B_{22}e^{-(n_2+n_8)y} - B_{23}e^{-(n_2+n_{10})y}$$

$$\theta_{02} = B_{49}e^{-n_{16}y} - B_{25}e^{-(n_{10}+n_{14})y} + B_{26}e^{-(n_{10}+n_{12})y} - B_{27}e^{-3n_{10}y} - B_{28}e^{-(2n_8+n_{10})y} - B_{29}e^{-(2n_2+n_{10})y} + B_{30}e^{-(n_8+2n_{10})y}$$
$$- B_{31}e^{-(n_2+n_8+n_{10})y} + B_{32}e^{-(n_2+2n_{10})y} + B_{33}e^{-(n_8+n_{14})y} - B_{34}e^{-(n_8+n_{12})y} + B_{35}e^{-(n_8+2n_{10})y} + B_{36}e^{-3n_8y} + B_{37}e^{-(2n_2+n_8)y}$$
$$- B_{38}e^{-(2n_8+n_{10})y} + B_{39}e^{-(n_2+2n_8)y} - B_{40}e^{-(n_2+n_8+n_{10})y} + B_{41}e^{-(n_2+n_{14})y} - B_{42}e^{-(n_2+n_{12})y} + B_{43}e^{-(n_2+2n_{10})y} + B_{44}e^{-(n_2+2n_8)y}$$
$$+ B_{45}e^{-3n_2y} - B_{46}e^{-(n_2+n_8+n_{10})y} + B_{47}e^{-(2n_2+n_8)y} + B_{48}e^{-(2n_2+n_{10})y}.$$

$$u_{02} = B_{75}e^{-n_{18}y} - B_{50}e^{-n_{16}y} + B_{51}e^{-(n_{10}+n_{14})y} - B_{52}e^{-(n_{10}+n_{12})y} + B_{53}e^{-3n_{10}y} + B_{54}e^{-(2n_8+n_{10})y} + B_{55}e^{-(2n_2+n_{10})y} - B_{56}e^{-(n_8+2n_{10})y}$$
$$+ B_{57}e^{-(n_2+n_8+n_{10})y} - B_{58}e^{-(n_2+2n_{10})y} - B_{59}e^{-(n_8+n_{14})y} + B_{60}e^{-(n_8+n_{12})y} - B_{61}e^{-(n_8+2n_{10})y} - B_{62}e^{-3n_8y} - B_{63}e^{-(2n_2+n_8)y}$$
$$+ B_{64}e^{-(2n_8+n_{10})y} - B_{65}e^{-(n_2+2n_8)y} + B_{66}e^{-(n_2+n_8+n_{10})y} - B_{67}e^{-(n_2+n_{14})y} + B_{68}e^{-(n_2+n_{12})y} - B_{69}e^{-(n_2+2n_{10})y} - B_{70}e^{-(n_2+2n_8)y}$$
$$- B_{71}e^{-3n_2y} + B_{72}e^{-(n_2+n_8+n_{10})y} - B_{73}e^{-(2n_2+n_8)y} - B_{74}e^{-(2n_2+n_{10})y}$$

$$\theta_{10} = e^{-n_{20}y}$$

$$u_{10} = B_{78}e^{-n_{22}y} - B_{76}e^{-n_{20}y} - B_{77}e^{-n_4y}$$

$$\theta_{11} = B_{97}e^{-n_{24}y} - B_{88}e^{-(n_{10}+n_{22})y} + B_{89}e^{-(n_{10}+n_{20})y} + B_{90}e^{-(n_4+n_{10})y} + B_{91}e^{-(n_8+n_{22})y} - B_{92}e^{-(n_8+n_{20})y} - B_{93}e^{-(n_4+n_8)y}$$
$$+ B_{94}e^{-(n_2+n_{22})y} - B_{95}e^{-(n_2+n_{20})y} - B_{96}e^{-(n_2+n_4)y}.$$

$$u_{11} = B_{108}e^{-n_{26}y} - B_{98}e^{-n_{24}y} + B_{99}e^{-(n_{10}+n_{22})y} - B_{100}e^{-(n_{10}+n_{20})y} - B_{101}e^{-(n_4+n_{10})y} - B_{102}e^{-(n_8+n_{22})y} + B_{103}e^{-(n_8+n_{20})y} + B_{104}e^{-(n_4+n_8)y}$$
$$- B_{105}e^{-(n_2+n_{22})y} + B_{106}e^{-(n_2+n_{20})y} + B_{107}e^{-(n_2+n_4)y}.$$

$$e^{-(n_2+n_4+n_{10})y} + B_{177}e^{-(n_8+n_{26})y} - B_{178}e^{-(n_8+n_{24})y} + B_{179}e^{-(n_8+n_{10}+n_{22})y} - B_{180}e^{-(n_8+n_{10}+n_{20})y} - B_{181}e^{-(n_4+n_8+n_{10})y} -$$
$$B_{182}e^{-(2n_8+n_{22})y} + B_{183}e^{-(2n_8+n_{20})y} + B_{184}e^{-(n_4+2n_8)y} - B_{185}e^{-(n_2+n_8+n_{22})y} + B_{186}e^{-(n_2+n_8+n_{20})y} + B_{187}e^{-(n_2+n_4+n_8)y} +$$
$$B_{188}\, e^{-(n_2+n_{26})y} - B_{189}e^{-(n_2+n_{24})y} + B_{190}e^{-(n_2+n_{10}+n_{22})y} - B_{191}e^{-(n_2+n_{10}+n_{20})y} - B_{192}e^{-(n_2+n_4+n_{10})y} - B_{193}e^{-(n_2+n_8+n_{22})y} +$$
$$B_{194}e^{-(n_2+n_8+n_{20})y} + B_{195}e^{-(n_2+n_4+n_8)y} - B_{196}e^{-(2n_2+n_{22})y} + B_{197}e^{-(2n_2+n_{20})y} + B_{198}e^{-(2n_2+n_4)y} - B_{199}e^{-(n_{14}+n_{22})y} +$$
$$B_{200}e^{-(n_{14}+n_{20})y} + B_{201}e^{-(n_4+n_{14})y} + B_{202}e^{-(n_{12}+n_{22})y} - B_{203}e^{-(n_{12}+n_{20})y} - B_{204}e^{-(n_{12}+n_4)y} - B_{205}e^{-(2n_{10}+n_{22})y} +$$
$$B_{206}e^{-(2n_{10}+n_{20})y} + B_{207}e^{-(n_4+2n_{10})y} - B_{208}e^{-(2n_8+n_{22})y} + B_{209}e^{-(2n_8+n_{20})y} + B_{210}e^{-(n_4+2n_8)y} - B_{211}e^{-(2n_2+n_{22})y} +$$
$$B_{212}e^{-(2n_2+n_{20})y} + B_{213}e^{-(2n_2+n_4)y} + B_{214}e^{-(n_8+n_{10}+n_{22})y} - B_{215}e^{-(n_8+n_{10}+n_{20})y} - B_{216}e^{-(n_4+n_8+n_{10})y} - B_{217}e^{-(n_2+n_8+n_{22})y}$$
$$+ B_{218}e^{-(n_2+n_8+n_{20})y} + B_{219}e^{-(n_2+n_4+n_8)y} + B_{220}e^{-(n_2+n_{10}+n_{22})y} - B_{221}e^{-(n_2+n_{10}+n_{20})y} - B_{222}e^{-(n_2+n_4+n_{10})y}$$

$$u_{12} = B_{282}e^{-n_{30}y} - B_{224}e^{-n_{28}y} + B_{225}e^{-(n_{10}+n_{26})y} - B_{226}e^{-(n_{10}+n_{24})y} + B_{227}e^{-(2n_{10}+n_{22})y} - B_{228}e^{-(2n_{10}+n_{20})y} -$$
$$B_{229}e^{-(n_4+2n_{10})y} - B_{230}e^{-(n_8+n_{10}+n_{22})y} + B_{231}e^{-(n_8+n_{10}+n_{20})y} + B_{232}e^{-(n_4+n_8+n_{10})y} - B_{233}e^{-(n_2+n_{10}+n_{22})y} + B_{234}e^{-(n_2+n_{10}+n_{20})y} +$$
$$B_{235}e^{-(n_2+n_4+n_{10})y} - B_{236}e^{-(n_8+n_{26})y} + B_{237}e^{-(n_8+n_{24})y} - B_{238}e^{-(n_8+n_{10}+n_{22})y} + B_{239}e^{-(n_8+n_{10}+n_{20})y} + B_{240}e^{-(n_4+n_8+n_{10})y} +$$
$$B_{241}e^{-(2n_8+n_{22})y} - B_{242}e^{-(2n_8+n_{20})y} - B_{243}e^{-(n_4+2n_8)y} + B_{244}e^{-(n_2+n_8+n_{22})y} - B_{245}e^{-(n_2+n_8+n_{20})y} - B_{246}e^{-(n_2+n_4+n_8)y} -$$
$$B_{247}\, e^{-(n_2+n_{26})y} - B_{245}e^{-(n_2+n_8+n_{20})y} - B_{246}e^{-(n_2+n_4+n_8)y} - B_{247}\, e^{-(n_2+n_{26})y} + B_{248}e^{-(n_2+n_{24})y} - B_{249}e^{-(n_2+n_{10}+n_{22})y} +$$
$$B_{250}e^{-(n_2+n_{10}+n_{20})y} + B_{251}e^{-(n_2+n_4+n_{10})y} + B_{252}e^{-(n_2+n_8+n_{22})y} - B_{253}e^{-(n_2+n_8+n_{20})y} - B_{254}e^{-(n_2+n_4+n_8)y} + B_{255}e^{-(2n_2+n_{22})y} -$$
$$B_{256}e^{-(2n_2+n_{20})y} - B_{257}e^{-(2n_2+n_4)y} + B_{258}e^{-(n_{14}+n_{22})y} - B_{259}e^{-(n_{14}+n_{20})y} - B_{260}e^{-(n_4+n_{14})y} - B_{261}e^{-(n_{12}+n_{22})y} +$$
$$B_{262}e^{-(n_{12}+n_{20})y} + B_{263}e^{-(n_{12}+n_4)y} + B_{264}e^{-(2n_{10}+n_{22})y} - B_{265}e^{-(2n_{10}+n_{20})y} - B_{266}e^{-(n_4+2n_{10})y} + B_{267}e^{-(2n_8+n_{22})y} -$$
$$B_{268}e^{-(2n_8+n_{20})y} - B_{269}e^{-(n_4+2n_8)y} + B_{270}e^{-(2n_2+n_{22})y} - B_{271}e^{-(2n_2+n_{20})y} - B_{272}e^{-(2n_2+n_4)y} - B_{273}e^{-(n_8+n_{10}+n_{22})y}$$
$$+ B_{274}e^{-(n_8+n_{10}+n_{20})y} + B_{275}e^{-(n_4+n_8+n_{10})y} + B_{276}e^{-(n_2+n_8+n_{22})y} - B_{277}e^{-(n_2+n_8+n_{20})y} - B_{278}e^{-(n_2+n_4+n_8)y}$$
$$- B_{279}e^{-(n_2+n_{10}+n_{22})y} + B_{280}e^{-(n_2+n_{10}+n_{20})y} + B_{281}e^{-(n_2+n_4+n_{10})y}$$

$$\theta_{20} = e^{-n_{32}y}$$

$$u_{20} = B_{283}e^{-n_{34}y} - B_{283}e^{-n_{32}y}$$

$$\theta_{21} = B_{302}e^{-n_{36}y} - B_{293}e^{-2n_{22}y} - B_{294}e^{-2n_{20}y} - B_{295}e^{-2n_4y} - B_{296}e^{-(n_{10}+n_{34})y} + B_{297}e^{-(n_{10}+n_{32})y} +$$
$$B_{298}e^{-(n_8+n_{34})y} - B_{299}e^{-(n_8+n_{32})y} + B_{300}e^{-(n_2+n_{34})y} - B_{301}e^{-(n_2+n_{32})y}$$

$$u_{21} = B_{313}e^{-n_{38}y} - B_{303}e^{-n_{36}y} + B_{304}e^{-2n_{22}y} + B_{305}e^{-2n_{20}y} + B_{306}e^{-2n_4y} + B_{307}e^{-(n_{10}+n_{34})y} -$$
$$B_{308}e^{-(n_{10}+n_{32})y} - B_{309}e^{-(n_8+n_{34})y} + B_{310}e^{-(n_8+n_{32})y} - B_{311}e^{-(n_2+n_{34})y} + B_{312}e^{-(n_2+n_{32})y}$$

$$\theta_{22} = B_{478}e^{-n_{40}y} - B_{396}e^{-(n_{22}+n_{26})y} + B_{397}e^{-(n_{22}+n_{24})y} - B_{398}e^{-(n_{10}+2n_{22})y} + B_{399}e^{-(n_{10}+n_{20}+n_{22})y} + B_{400}e^{-(n_4+n_{10}+n_{22})y} + B_{401}e^{-(n_8+2n_{22})y} - B_{402}e^{-(n_8+n_{20}+n_{22})y} - B_{403}e^{-(n_4+n_8+n_{22})y} + B_{404}e^{-(n_2+2n_{22})y} - B_{405}e^{-(n_2+n_{20}+n_{22})y} - B_{406}e^{-(n_2+n_4+n_{22})y} + B_{407}e^{-(n_{20}+n_{26})y} - B_{408}e^{-(n_{20}+n_{24})y} + B_{409}e^{-(n_{10}+n_{20}+n_{22})y} - B_{410}e^{-(n_{10}+2n_{20})y} - B_{411}e^{-(n_4+n_{10}+n_{20})y} - B_{412}e^{-(n_8+n_{20}+n_{22})y} + B_{413}e^{-(n_8+2n_{20})y} + B_{414}e^{-(n_4+n_8+n_{20})y} - B_{415}e^{-(n_2+n_{20}+n_{22})y} + B_{416}e^{-(n_2+2n_{20})y} + B_{417}e^{-(n_2+n_4+n_{20})y} + B_{418}e^{-(n_4+n_{26})y} - B_{419}e^{-(n_4+n_{24})y} + B_{420}e^{-(n_4+n_{10}+n_{22})y} - B_{421}e^{-(n_4+n_{10}+n_{20})y} - B_{422}e^{-(2n_4+n_{10})y} - B_{423}e^{-(n_4+n_8+n_{22})y} + B_{424}e^{-(n_4+n_8+n_{20})y} + B_{425}e^{-(2n_4+n_8)y} - B_{426}e^{-(n_2+n_4+n_{22})y} + B_{427}e^{-(n_2+n_4+n_{20})y} + B_{428}e^{-(n_2+2n_4)y} - B_{429}e^{-(n_{10}+n_{38})y} + B_{430}e^{-(n_{10}+n_{36})y} - B_{431}e^{-(n_{10}+2n_{22})y} - B_{432}e^{-(n_{10}+2n_{20})y} - B_{433}e^{-(2n_4+n_{10})y} - B_{434}e^{-(2n_{10}+n_{34})y} + B_{435}e^{-(2n_{10}+n_{32})y} + B_{436}e^{-(n_8+n_{10}+n_{34})y} - B_{437}e^{-(n_8+n_{10}+n_{32})y} + B_{438}e^{-(n_2+n_{10}+n_{34})y} - B_{439}e^{-(n_2+n_{10}+n_{32})y} + B_{440}e^{-(n_8+n_{38})y} - B_{441}e^{-(n_8+n_{36})y} + B_{442}e^{-(n_8+2n_{22})y} + B_{443}e^{-(n_8+2n_{20})y} + B_{444}e^{-(2n_4+n_8)y} + B_{445}e^{-(n_8+n_{10}+n_{34})y} - B_{446}e^{-(n_8+n_{10}+n_{32})y} - B_{447}e^{-(2n_8+n_{34})y} + B_{448}e^{-(2n_8+n_{32})y} - B_{449}e^{-(n_2+n_8+n_{34})y} + B_{450}e^{-(n_2+n_8+n_{32})y} + B_{451}e^{-(n_2+n_{38})y} - B_{452}e^{-(n_2+n_{36})y} + B_{453}e^{-(n_2+2n_{22})y} + B_{454}e^{-(n_2+2n_{20})y} + B_{455}e^{-(n_2+2n_4)y} + B_{456}e^{-(n_2+n_{10}+n_{34})y} - B_{457}e^{-(n_2+n_{10}+n_{32})y} - B_{458}e^{-(n_2+n_8+n_{34})y} + B_{459}e^{-(n_2+n_8+n_{32})y} - B_{460}e^{-(2n_2+2n_{34})y} + B_{461}e^{-(2n_2+n_{32})y} - B_{462}e^{-(n_{14}+n_{34})y} + B_{463}e^{-(n_{14}+2n_{32})y} + B_{464}e^{-(n_{12}+n_{34})y} - B_{465}e^{-(n_{12}+n_{32})y} - B_{466}e^{-(2n_{10}+n_{34})y} + B_{467}e^{-(2n_{10}+n_{32})y} - B_{468}e^{-(2n_8+n_{34})y} + B_{469}e^{-(2n_8+n_{32})y} - B_{470}e^{-(2n_2+n_{34})y} + B_{471}e^{-(2n_2+n_{32})y} + B_{472}e^{-(n_8+n_{10}+n_{34})y} - B_{473}e^{-(n_8+n_{10}+n_{32})} - B_{474}e^{-(n_2+n_8+n_{34})y} + B_{475}e^{-(n_2+n_8+n_{32})y} + B_{476}e^{-(n_2+n_{10}+n_{34})y} - B_{477}e^{-(n_2+n_{10}+n_{32})y}$$

From Eq. (14), we get the real expressions for velocity and temperature profiles as;

$$f(y,z,t) = f_0(y) + \in [f_r \cos(\pi z - t) - f_i \sin(\pi z - t)] + \in^2 [f_r \cos 2(\pi z - t) - f_i \sin 2(\pi z - t)] \tag{50}$$

where $f_1 = f_r + if_i$, $f_2 = f_r + if_i$

Skin-friction:

Knowing the velocity field, the expression for the skin-friction coefficient at the plate in the X*-direction is given by

$$C_{fx} = \left(\frac{\partial u}{\partial y}\right)_{y=0} \tag{51}$$

Nusselt number

From the temperature field, the rate of heat transfer coefficient in terms of the Nusselt number Nu at the plate is given by

$$Nu = \left(\frac{\partial \theta}{\partial y}\right)_{y=0} \tag{52}$$

Sherewood number

Knowing the concentration field, the rate of species concentration co-efficient in terms of the Sherwood number Sh at the plate is given by

$$Sh = \left(\frac{\partial C}{\partial y}\right)_{y=0} \tag{53}$$

4 Results and discussion

Numerical evaluation of the analytical results obtained in the preceding section is represented quantitatively and discussed qualitatively through Figs. 2-14, in which the influence of various flow field parameters such as Schmidh number, Reynolds number, Gamma, Prandtl number, Radiation parameter, Grashof number, Eckert number, solutal Grashof number are shown on velocity(U), Temperature (Θ) and concentration (C) distributions. The validity of the present work is displayed through comparative study in Tab. 1. The numerical values of skin-friction, Nusselt number and Sherwood number obtained in the present case are compared with those of Sarangi et al. [Sarangi and Jose (2005)] for different values of Prandtl number (*Pr)* and fixed values of remaining parameters. It is clearly seen that there is an excellent agreement between the respective research of our study and those of Sarangi et al. [Sarangi and Jose (2005)]

Fig. 2 displays the influence of species concentration for different values of Schmidt's number Sc. Physically, Schmidt number is the ratio of momentum diffusivity to molecular diffusivity. $Sc = 1$ indicates that the both diffusion rates are of the same order. $Sc > 1$ implies momentum diffusivity rate exceeds the molecular diffusivity and vice versa for $Sc < 1$. It is seen that as Sc is incremented the species concentration gets diluted and the thickness of the associated boundary layers is reduced. These results are in good agreement with the results of Paras et al. [Paras, Hawa, Rakesh et al. (2017)]. Also, the rate of mass transfer of a fluid in ammonia (Sc=78) is more than that of water (Sc=60). Ammonia also known as Azane is a colorless gas with a characteristic pungent smell. It is also used in many commercial cleaning products. The effect of Reynolds number *Re* on the concentration is illustrated field in Fig. 3. As the Reynolds number increases the concentration is found to be decreasing. It is noticed that the mass transfer of a fluid at initial stage is high and later it converges to the boundary layer.

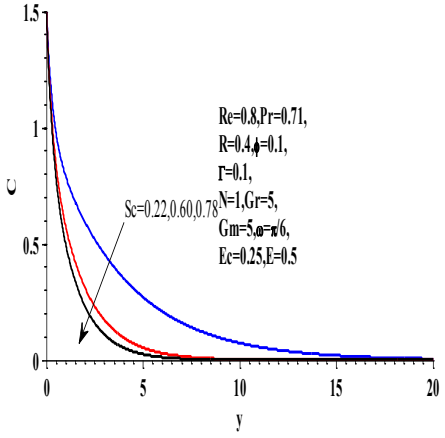

Figure 2: Effect of *Sc* on concentration profiles

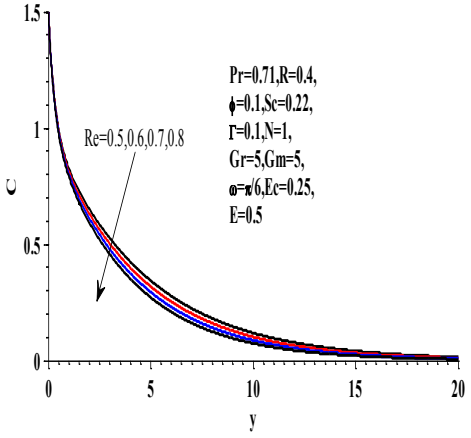

Figure 3: Effect of *Re* on concentration profiles

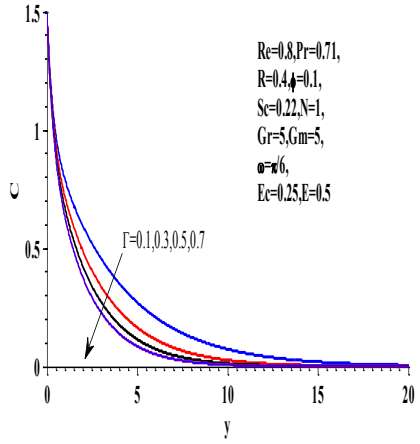

Figure 4: Effect of Γ on concentration profiles

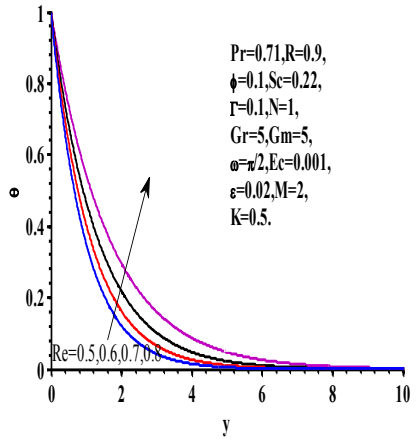

Figure 5: Effect of *Re* on temperature profiles

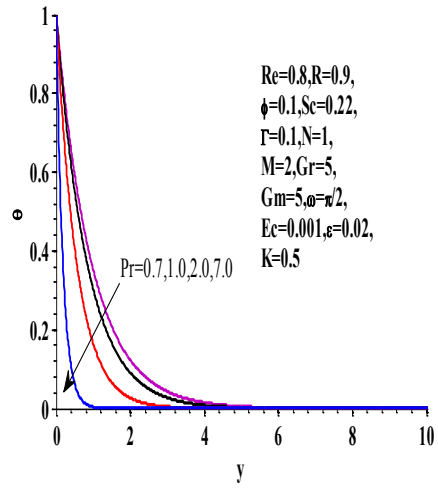

Figure 6: Effect of *Pr* on temperature profiles

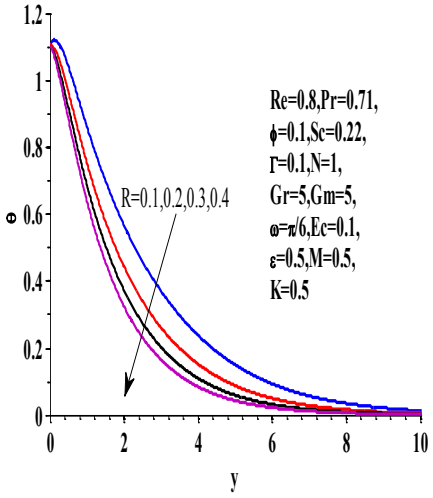

Figure 7: Effect of *R* on temperature profiles

The effects of chemical reaction on concentration profiles is presented in Fig. 4. It is observed that the concentration of fluid at the surface reduces on increasing the chemical reaction parameters. The influence of the Reynolds number on temperature profile against spanwise coordinates is displayed in Fig. 5. It is noticed that the temperature increases with the rising values of *Re* across the boundary layer.

Fig. 6 shows the variation of Prandtl number (Pr) on temperature. It is seen that increasing values of Prandtl number shows a drop in temperature. Physically an increase in Pr amounts to smaller values of the thermal conductivity and hence the temperature tends to decrease, i.e., the temperature of fluids with higher Prandtl number drops rapidly. Also, the magnitude of temperature for air (Pr=0.7) is better than that of water (Pr=7). Fig.

7 illustrates the effect of *R* on the temperature distributions. It is obvious that as R increases, the Θ decreases. Also, it is noticed that the Θ has peak value at the wall (y=0) across the boundary layer.

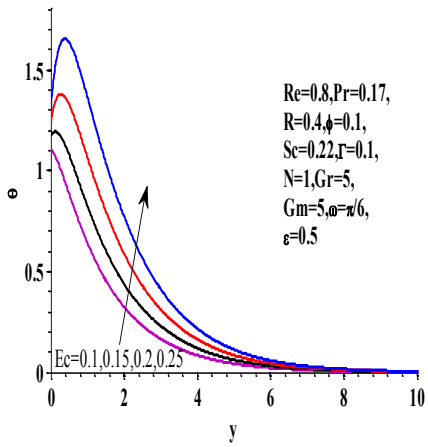

Figure 8: Effect of *Ec* on temperature profiles

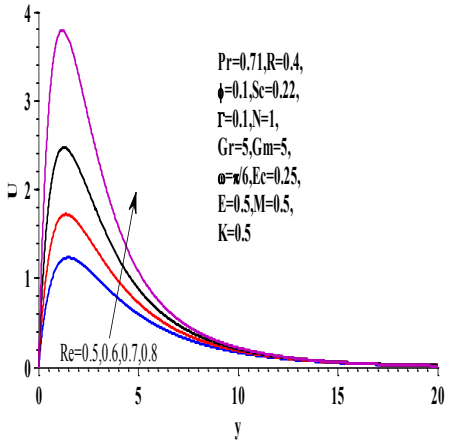

Figure 9: Effect of *Re* on velocity profiles

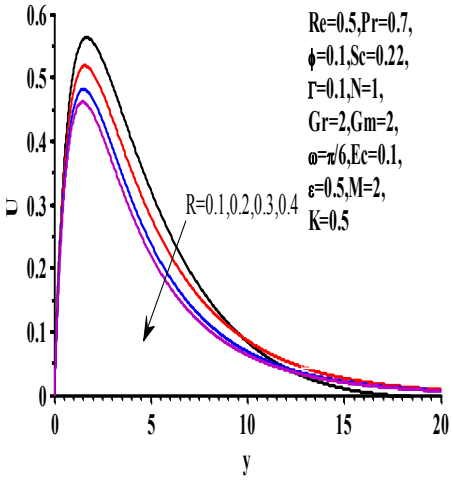

Figure 10: Effect of *R* on velocity profiles

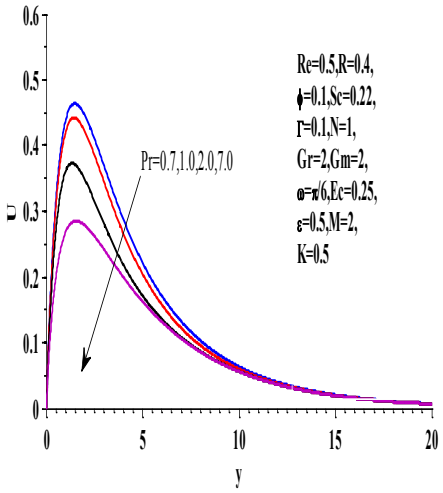

Figure 11: Effect of *Pr* on velocity profiles

The influence of *Ec* on Θ is displayed in Fig. 8. It is obvious that Θ increases with the rise of Ec values. This is due to this fact, the thermal boundary layer becomes thicker and diminishes the temperature dissipation from plate to the fluid which causes heat up of the plate. Figs. 9 and 10 depict the dimensionless velocity profile for different values of Re and R respectively. It is noticed that velocity profile increase with increasing values of Re

and decrease with rising values of R. Physically, large values of *R* correspond to a momentum boundary layer, hence *R* leads to decreasing the fluid boundary layer.

The effect of Prandtl number on U is presented in Fig. 11. It is noticed that U at the surface reduces on increasing *Pr* values. This is because, the momentum boundary layer thickness is thinning more rapidly due to the thermal diffusion of the fluid particles.

The effects of *Gr* and *Gm* on velocity distribution is presented in Figs. 12 and 13 respectively. It is noticed that the velocity increases near the plate and after attaining its peak value, it decreases and finally converges to its boundary value. As expected, the fluid velocity increases and the peak value becomes more distinctive due to increase in the buoyancy forces. The effect of *Ec* on the velocity is shown in Fig. 14. Greater viscous dissipative heat causes a rise in the velocity.

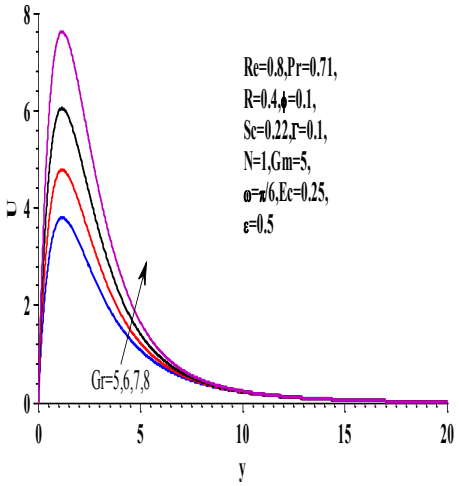

Figure 12: Effect of *Gr* on velocity profiles

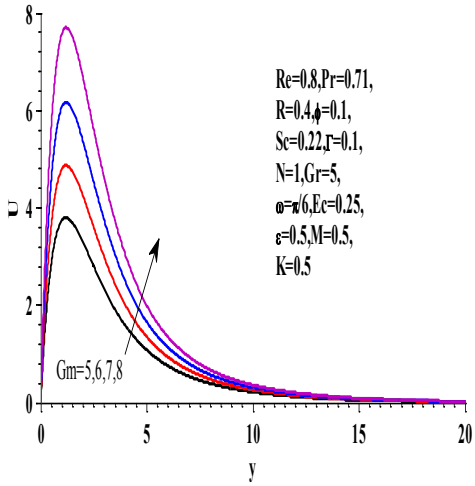

Figure 13: Effect of *Gm* on velocity profiles

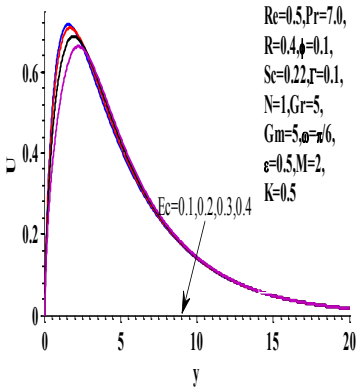

Figure 14: Effect of *Ec* on velocity profiles

Table 1: Comparison of present results (C_f, *Nu* and *Sh)* with those of Sarangi et al. [Sarangi and Jose (2005)] for different values of Pr

Pr	Sarangi et al. [Sarangi and Jose (2005)]			Present results		
	C_f	*Nu*	*Sh*	C_f	*Nu*	*Sh*
0.1	9.7825	-1.7881	-2.6	9.7868	-1.7878	-2.2611
0.2	8.0855	-3.5914	-2.6	8.0858	-3.5925	-2.2611
0.3	7.2119	-5.3985	-2.6	7.2127	-5.3988	-2.2611
0.4	6.6769	-7.2116	-2.6	6.6781	-7.2120	-2.2611

Table 2: Skin friction coefficients for different values of Re, Gr, Gm, N

Re	Gr	Gm	N	C_f
0.5	2	2	1	2.1334
1				8.4063
2				31.0159
3				62.2796
	3			2.6467
	4			3.1603
	5			3.6746
		3		2.6877
		4		3.2422
		5		3.7967
			2	1.5993
			3	1.3546
			4	1.2067

Tabs. 2, 3 and 4 display the influence of various flow parameters on skinfriction coefficient, Nusselt number and rate of mass transfer respectively by considering the following values

$$\in = 0.02, \gamma = 0.1, \omega = 5, t = \frac{\pi}{2}, R = 0.5,\ K = 0.5\ ,\ \mathrm{Pr} = 0.71, \mathrm{Re} = 2,\ Ec = 0.001,\ and\ z = 0$$

It is observed that C_f and S_h rise with growing values of Re, Sc, Gm, Γ and opposite trend is noticed in case of *Nu* with intensifying values of Pr, Re and Ec.

Table 3: Rate of Heat transfer coefficient (Nusselt Number) for different values of Pr, RE, Ec, R

Pr	Re	Ec	R	ϕ	Nu
0.10	0.5	0.1	0.4	0.1	4.1158
0.70					4.321
1.00					4.4578
0.10	3				5.3509
	4				5.2547
	5				4.9423
		0.2			3.6252
		0.3			2.9251
		0.4			2.8899
			0.5		4.1584
			0.6		4.1967
			0.7		4.232
				0.2	4.0974
				0.3	4.0778
				0.4	4.0568

Table 4: Rate of mass Transfer coefficient (Sherwood number) for different values of Re, Sc, C

Re	Sc	Γ	*Sh*
3	0.22	0.1	3.1611
4			3.4608
5			3.766
0.5	0.60		2.7738
	0.78		2.9078
	0.96		3.0403
		0.2	2.5373
		0.3	2.5856
		0.4	2.6271

5 Conclusions

In this paper, we tend to analyse the chemical reaction and thermal radiation effects past a porous vertical plate with cosinusoidally unsteady boundary conditions. The governing equations are solved analytically by perturbation technique. The result of assorted parameters on the momentum, thermal and concentration as well as the Skin-friction, the rate of heat and mass transfer coefficients, discussed and displayed through graphs and tables. The following conclusions are drawn from the present study.

- The velocity profiles increase with increasing values of Gr and Gm.
- The increasing values of Pr, Re and R decelerate both the transient velocity and temperature of the flow field at all points.
- The Concentration decreases with increasing values of the chemical reaction parameter, Schmidt number and the Reynolds number Re
- The rate of heat transfer decreases with increasing values of Pr and Ec.

It is hoped that the findings of this investigation may be useful for applications in power engineering, geothermal energy extractions, but also serve as a complement to the previous studies.

References

Ahmed, N.; Talukdar, S. (2011): Oscillatory MHD flow past a porous plate in a rotating system with periodic suction. *Thermal Engineering*, vol. 32, pp. 2007-2012.

Ahmed, S.; Zueco, J.; Lopez-Gonzalez, L. M. (2017): Effects of chemical reaction, heat and mass transfer and viscous dissipation over a MHD flow in a vertical porous wall using Perturbation method. *International Journal of Heat and Mass Transfer*, vol. 104, pp. 409-418.

Anu Radha, S. (2014): Heat and mass transfer of oscillatory free convective MHD flow past an infinite vertical porous plate with cosinusoidally fluctuating temperature. *International Seminar in Advances in Applied Mathematics.*

Arifuzzaman, S. M.; Khan, M. S.; Mehedi, M. F. U.; Rana, B. M. J.; Ahmmed, S. F. (2018): Chemically reactive and naturally convective high speed MHD fluid flow through an oscillatory vertical porous plate with heat and radiation absorption effect. *Engineering Science and Technology, an International Journal*, vol. 21, pp. 215-228.

Asma, K.; Khan, L.; Sharidan, S. (2016): Heat transfer in Ferro-fluid with cylindrical shape nano particles past a vertical plate with ramped wall temperature embedded in a porous medium. *Journal of Molecular Liquids*, vol. 221, pp. 1175-1183.

Bakr, A. A. (2011): Effects of chemical reaction on MHD free convection and mass transfer flow of a micro polar fluid with oscillatory plate velocity and constant heat source in a rotating frame of reference. *Communications in Nonlinear Science and Numerical Simulation*, vol. 16, pp. 698-710.

Balla, C. S.; Kishan, N. (2015): Radiation effects on unsteady MHD convective heat and mass transfer past a vertical plate with chemical reaction and viscous dissipation. *Alexandria Engineering Journal*, vol. 54, pp. 661-671.

Chamka, A. J. (2014): Unsteady MHD convective heat and mass transfer past a semi infinite vertical plate with heat absorption. *International Journal of Engineering Science*, vol. 42, no. 2, pp. 217-230.

Chamkha, A. J.; Mohamed, R. A.; Ahmed, S. E. (2011): Unsteady MHD natural convection from a heated vertical porous plate in a micro polar fluid with Joule heating chemical reaction and radiation effects. *Meccanica*, vol. 46, pp. 399-411.

Das, S.; Guchhait, S. K.; Jana, R. N.; Makinde, O. D. (2016): Hall effects on an unsteady magneto-convection and radiative heat transfer past a porous plate. *Alexandria Engineering Journal*, vol. 55, pp. 1321-1331.

Harish Babu, D.; Satya Narayana, P. V. (2016): Joule heating effects on MHD mixed convection of a Jeffrey fluid over a stretching sheet with power law heat flux: a numerical study. *Journal of Magnetism and Magnetic Materials*, vol. 412, pp. 185-193

Hussain, S. M.; Jain, J.; Seth, G. S.; Rashidi, M. M. (2015): Free Convective heat transfer with hall effects, heat absorption and chemical reaction over an accelerated moving plate in a rotating system. *Journal of Magnetism and Magnetic Materials*, vol. 422, pp. 112-123.

Makinde, O. D.; Khan, W. A.; Khan, Z. H. (2016): Stagnation point flow of MHD chemically reacting nano fluid over a stretching convective surface with slip and radiative heat. *Proceedings of the Institution of Mechanical Engineers, Part E: Journal of Process Mechanical Engineering*, vol. 231, no. 4.

Mondal, H.; Dulal, P.; Sewli, C.; Precious, S. (2017): Thermophoresis and Soret-Dufour on MHD mixed convection mass transfer over an inclined plate with non-uniform heat source/sink and chemical reaction. *Ain Shams Engineering Journal*, vol. 9, no. 4, pp. 2111-2121.

Muthuraj, R.; Nirmala, K.; Srinivas, S. (2016): Influences of chemical reaction and wall properties on MHD peristaltic transport of a Dusty fluid with Heat and Mass transfer. *Alexandria Engineering Journal*, vol. 55 pp. 597-611.

Nandkeolyar, R.; Das, M. (2013): Unsteady MHD free convection flow of a heat absorbing dusty fluid past a flat plate with ramped wall temperature. *Afrika Matmateika*, vol. 25, pp. 79-98.

Nayak, M. K.; Dash, G. C.; Singh, L. P. (2016): Heat and Mass Transfer effects on MHD Viscoelastic fluid over a stretching sheet through porous medium in presence of chemical reaction. *Propulsion and Power Research*, vol. 5, pp. 70-80.

Paras, R.; Hawa, S.; Rakesh, K.; Vikas, K.; Vimal Kumar, J. (2017): Free convective boundary layer flow of radiation and reacting MHD fluid past a cosinusoidally fluctuating heated plate. *International Journal of Applied Mathematics and Computer Science*, vol. 3, pp. 261-294.

Rama Krishna Reddy, P.; Raju, M. C. (2018): MHD free convective flow past a porous plate. *International Journal of Pure and Applied Mathematics*, vol. 118, pp. 507-529.

Rana, S.; Mehmood, I. R.; Narayana, P. V. S.; Akbar, N. S. (2016): Free convective nonaligned non-Newtonian flow with non-linear thermal radiation. *Communications in Theoretical Physics*, vol. 66, pp. 687-693.

Ravikumar, V.; Raju, M. C.; Raju, G. S. S. (2018): Combined effects of heat absorption and MHD on convective Rivlin-Ericksen flow past a semi-infinite vertical porous plate with variable temperature and suction. *Ain Shams Engineering Journal*, vol. 5, pp. 867-875.

Sarangi, K. C.; Jose, C. B. (2005): Unsteady free convective MHD flow and mass transfer past a vertical porous plate with variable temperature. *Bulletin of the Malaysian Mathematical Sciences Society*, vol. 97, no. 2, pp. 137-146.

Sarojamma, G.; Vijaya Lakshmi, R.; Satya Narayana, P. V.; Makinde, O. D. (2018): Non-linear radiative flow of a micropolar nano fluid through a vertical channel with porous collapsible walls. *Defect Diffusion Forum*, vol. 387, pp. 498-509.

Satya Narayan, P. V.; Tarakaramu, N.; Makinde, O. D.; Venkateswarlu, B.; Sarojamma, G. (2018): MHD stagnation point flow of viscoelastic nanofluid past a convectively heated stretching surface. *Defect Diffusion Forum*, vol. 387, pp. 106-120.

Satya Narayana, P. V.; Akshit, S. M.; Ghori, J. P.; Venkateswarlu, B. (2017): Thermal radiation effects on an unsteady MHD nanofluid flow over a stretching sheet with non-uniform heat source/sink. *Journal of Nanofluids*, vol. 8, pp. 1-5.

Satya Narayana, P. V.; Harish Babu, D. (2013): MHD free convective heat and mass transfer past a vertical porous plate with variable temperature. *International Journal of Applied Mathematics and Computer Science*, vol. 9, no. 7, pp. 66-94.

Seshaiahand, B.; Varma, S. V. K. (2016): Chemical reaction effects on MHD free convective flow through porous medium with constant suction and heat flux. *International Journal of Applied Ceramic Technology*, vol. 3 pp. 340-355.

Seth, G. S.; Sarkar, S.; Hussain, S. M. (2014): Effects of Hall current, radiation and rotation on natural convection heat and mass transfer flow past a moving vertical plate. *Ain Shams Engineering Journal*, vol. 5, pp. 489-503.

Seth, G. S.; Sharma, R.; Kumbhakar, B. (2016): Heat and mass transfer effects on unsteady MHD natural convection flow of a chemically reactive and radiating fluid through a porous medium past a moving vertical plate with arbitrary ramped temperature, *Journal of Applied Fluid Mechanics*, vol. 9, no. 1, pp. 103-117.

Singh, H.; Ram, P.; Kumar, V. (2014): Unsteady MHD free convection past an impulsively started vertical plate with radiation and viscous dissipation. *Fluid Dynamics & Materials Processing*, vol. 10, no. 4, pp. 521-550.

Soid, S. K.; Ishak, A.; Pop, I. (2017): Unsteady MHD flow and heat transfer over a shrinking sheet with ohmic heating. *Chinese Journal of Physics*, vol. 55, no. 4, pp. 1626-1636.

Swathi, M.; Iswar, C. M. (2015): Magnetohydrodynamic (MHD) mixed convection slip flow and heat transfer over a vertical porous plate. *Engineering Science and Technology an International Journal*, vol. 18, pp. 98-105.

Venkateshwarlu, B.; Satyanarayana, P. V. (2015): Chemical reaction and radiation absorption effects on the flow and heat transfer of a nanofluid in a rotating system. *Applied Nano Science*, vol. 4, no. 3, pp. 351-360.

Vincenti, W. G.; Krugger, C. H. (1965): *Introduction to Physical Gas Dynamics*. Wiley, New York.